Supporting Information

Kerr *et al.* 10.1073/pnas.0800621105

SI Text

Organotypic Slice Culture. Stoppini-type interface organotypic slice cultures (1) were prepared from the brains of wild-type (+/+) or synaptotagmin 1 knockout (−/−) newborn mice (strain: B6,129S-Syt1^{tm1Sud}/J; The Jackson Laboratory). Wild-type and knockout mice were taken from the same mouse colony, typically from the same litters. Animals were killed by decapitation, in agreement with national and institutional guidelines. The hippocampus, still attached to the entorhinal cortex, was removed and placed in cold Hanks' balanced salt solution (HBSS; Invitrogen) under sterile conditions. Slices of 300-μm thickness were cut perpendicularly to the longitudinal axis of the hippocampus with a McIllwain tissue chopper and placed on microporous membrane inserts (Millipore). Slices were maintained with culture medium, consisting of 50% minimum essential medium, 25% horse serum, 25% basal medium Eagle, 2 mM glutamax and 0.62% glucose (all from Invitrogen or Braun). At 3–5 days *in vitro* (DIV) 100 μM cytosine arabinoside, 100 μM uridine, and 100 μM 5-fluorodeoxyuridine (Sigma–Aldrich), dissolved in culture medium, were added for 24 h. Slice cultures were maintained at 37°C and in 5% CO_2 throughout incubation. Culture medium was changed 2–3 times per week, and cultures were used for recording between 16 and 29 DIV. The genotype of all animals used for slice cultures was determined using tail biopsy and subsequent PCR analysis (2) (Table S2).

Paired Recordings. Slice cultures were superfused with physiological saline, containing 125 mM NaCl, 25 mM $NaHCO_3$, 25 mM glucose, 2.5 mM KCl, 1.25 mM NaH_2PO_4, 2 mM $CaCl_2$, and 1 mM $MgCl_2$ (unless specified differently) at a flow rate of ≈3.5 ml min^{-1}. For deconvolution analysis of GC–BC EPSCs, 0.75 or 1 mM kynurenic acid was added to reduce the probability of polysynaptic events. Patch pipettes (resistance 2–5 MΩ, when filled with intracellular solution) were pulled from borosilicate glass tubing. The intracellular solution for presynaptic neurons and postsynaptic BCs contained 135 mM potassium gluconate, 20 mM KCl, 2 mM $MgCl_2$, 2 mM Na_2ATP, 0.1 mM EGTA, 10 mM Hepes, and 0.2% biocytin. The intracellular solution for postsynaptic GCs contained 110 mM KCl, 35 mM potassium gluconate, 2 mM $MgCl_2$, 2 mM Na_2ATP, 10 mM EGTA, 10 mM Hepes, 2 mM QX-314 (unless specified differently), and 0.2% biocytin (pH adjusted to 7.2 with KOH in both cases). Paired recordings were obtained from closely spaced BCs and GCs in the dentate gyrus under visual control by using infrared differential interference contrast videomicroscopy (Fig. S1). BCs were identified based on their fast spiking action potential (AP) phenotype, generating >50 APs during 1-s depolarizing current pulses (Fig. S1*D*). Two Axopatch 200A amplifiers (Molecular Devices) were used for current- and voltage-clamp recording. Presynaptic neurons were held in current clamp (I-Clamp normal), and APs were elicited by brief current pulses of 2- to 4-ms duration and 1.2- to 1.8-nA amplitude. Stimuli were applied every 10 s (for BC–GC connections) or every 30 s (for GC–BC connections) when 50-Hz trains of 10 stimuli were used and every 5 s when single stimuli were applied. In BC–GC IPSC recordings, postsynaptic GCs were held in at −80 mV; series resistance ($R_s \leq 15$ MΩ) was continuously monitored using 5-mV test pulses, but not compensated. In GC–BC EPSC recordings, postsynaptic BCs were held at −70 mV; series resistance ($R_s \leq 15$ MΩ) was monitored between recordings and compensated by ≈85% with ≈35-μs lag. Signals were filtered at 5 kHz and digitized at 40 kHz by using a CED 1401plus interface (Cambridge Electronic Design). Pulse generation and data acquisition were performed by using FPulse (U. Fröbe, Physiological Institute, Freiburg, Germany) running under IGOR Pro 5.04b (Wavemetrics) on a personal computer. GC–BC pairs in synaptotagmin 1-deficient mice were considered synaptically connected if a 50-Hz train of 10 APs led to a significant increase in EPSC frequency. The recording temperature was 23.8 ± 0.9°C (mean ± standard deviation).

Recording of Miniature EPSCs (mEPSCs) and Miniature IPSCs (mIPSCs). mEPSCs and mIPSCs were recorded in BCs and GCs at holding potentials of −70 mV and −80 mV, respectively, in the presence of 1 μM tetrodotoxin (TTX; Alomone). mEPSCs were pharmacologically isolated by bath application of 10 μM bicuculline methiodide (Tocris). mIPSCs were recorded in the presence of 10 μM 6-cyano-7-nitroquinoxaline-2,3-dione (CNQX; Tocris) and 20 μM D-2-amino-5-phosphonopentanoic acid (D-AP5; Tocris). For all miniature PSC recordings, series resistance ($R_s \leq 15$ MΩ) was compensated by ≈85% with ≈35-μs lag.

Data Analysis. Data were analyzed with FEval (U. Fröbe) running under IGOR, custom-built functions in IGOR, or Mathematica 4 or 5 (Wolfram Research). BC–GC pairs were only included in the study if the average peak amplitude of the evoked IPSCs was >100 pA. Latency, standard deviation of latency, amplitude, 20–80% rise time, and percentage of failures of evoked PSCs were determined as described (3, 4). If a train of stimuli was applied, analysis was performed on the first PSC. The decay time constant of PSCs was analyzed by fitting the decay of single events with a monoexponential function. Coefficient of variation and skewness were determined from PSC peak amplitudes including failures. Average traces were generated from 50 single sweeps. To quantify multiple-pulse depression of IPSCs, the amplitudes of the second and all subsequent IPSCs in the train were measured after iterative subtraction of the fitted decay phases of the preceding IPSCs (Fig. 2*B*).

To determine the time course of release after a single presynaptic AP, the distribution of first quantal latencies was measured under conditions of reduced release probability ($[Ca^{2+}]$ = 0.5 mM and $[Mg^{2+}]$ = 2.5 mM for wild-type and $[Ca^{2+}]$ = 1.0 mM and $[Mg^{2+}]$ = 2.0 mM for knockout cultures) and converted into the time course of release by using the method of Barrett and Stevens (3–5). Differences in the time course of release were examined by bootstrap procedures. One thousand artificial datasets were generated from the means and SEMs of the original dataset and analyzed as the original (6). For deconvolution analysis, average unitary PSCs were deconvolved from average quantal PSCs, and the proportions of synchronous release, asynchronous release during the train, and asynchronous release after the train were quantified as described previously, using the mean release rate 15–20 ms after each AP to quantify asynchronous release during the train (Fig. 3*F Inset*) (7). For deconvolution of GC–BC EPSCs, average quantal EPSC amplitude was multiplied by a correction factor (0.38), which was obtained as the ratio of block of spontaneous and evoked EPSCs by 0.75 mM kynurenic acid (A.M.K., unpublished data). For display purposes, release rates were filtered digitally (0.4 kHz for EPSCs, 4 kHz for IPSCs).

Quantal PSCs were detected by using a two-pass sliding template algorithm (8, 9). Events were detected based on predefined criteria for the correlation coefficient ($r_{crit} \geq 0.8$ for EPSCs and >0.85 for IPSCs). The template was specified as a

function with exponential rise and decay in the first pass and as the average quantal PSC waveform in the second pass.

mEPSCs and mIPSCs were detected with a similar sliding template approach, using $r_{crit} \geq 0.5$ or 0.6 and a critical amplitude of $a_{crit} \geq 30$ pA or 20 pA, respectively. The total recording time analyzed was 600–1,000 s.

Data are given as mean ± SEM. Error bars in figures also represent the SEM. Statistical significance was assessed by using nonparametric Mann–Whitney or Kruskal–Wallis tests at the significance level (P) indicated. In the figures, * corresponds to $P < 0.05$, ** to $P < 0.01$, and *** to $P < 0.001$.

Biocytin Staining and Immunocytochemistry. For analysis of neuron morphology after recording, slice cultures were fixed overnight in 2.5% paraformaldehyde, 1.25% glutaraldehyde, and 15% picric acid in 100 mM phosphate buffer (PB), pH 7.3. After fixation, the tissue was removed from the microporous membrane with a scalpel and treated with PB containing 1% avidin-biotinylated horseradish peroxidase complex (ABC; Vector Laboratories) and 0.1% Triton X-100 for 24 h at 4°C. Excess ABC was removed by several rinses in PB and finally in 50 mM Tris buffer (TB), before development with 0.05% 3,3′-diaminobenzidine tetrahydrochloride and 0.01% hydrogen peroxide in TB. Subsequently, slices were rinsed in TB several times and embedded in Mowiol (Höchst).

For immunocytochemistry, slice cultures were fixed overnight in 4% paraformaldehyde in PB. After wash in PB, the tissue was removed from the microporous membrane with a scalpel and washed several times in PBS (PBS, 150 mM NaCl in 100 mM PB). Slices were further washed for 1 h in PBS containing 10% normal goat serum and then processed in PBS containing 5% normal goat serum and 0.3% Triton X-100 for 24 h at room temperature with either polyclonal antibodies for parvalbumin (PV, rabbit, 1:1,000; Swant) in combination with rhodamine red-conjugated avidin-D (Fig. S1*D*) or polyclonal antibodies for PV (rabbit, 1:1,000, Swant) in combination with monoclonal antibodies for calbindin (mouse D28K, 1:1000; Swant, Fig. S1*B*). Secondary antibodies (goat anti-rabbit Alexa Fluor 488, goat anti-mouse Alexa Fluor 568, both at 1:500; Invitrogen) were applied with or without rhodamine red-conjugated avidin-D (1:500; Vector Laboratories), as required, in PBS containing 3% normal goat serum and 0.3% Triton X-100 for 24 h at 4°C. After wash, slices were embedded in Prolong Antifade Gold (Invitrogen). Control experiments in which the primary antibody was omitted gave consistently negative results.

Single-Cell RT-qPCR analysis. Single-cell expression analysis was performed by using reverse transcription (RT) followed by a multiplex PCR with 15 cycles and a subsequent quantitative PCR (RT-qPCR), as described (10, 11). RT-qPCR analysis was performed on cells in either acute slices from 18-day-old rats (Fig. 5*B*) or organotypic slice cultures from mice (Fig. 5*C*). The internal solution contained 140 mM KCl, 5 mM Hepes, 5 mM EGTA, and 3 mM $MgCl_2$ (pH adjusted to 7.3 with KOH) and was autoclaved before use. Patch-clamp capillaries were heated for 4 h at 220°C before use. After determining the AP phenotype of the recorded BC or GC in the whole-cell configuration, the cytoplasm was harvested into the recording pipette. Experiments in which the gigaseal was disrupted were discarded. Pipettes were then removed from the bath solution, reimmersed, and examined microscopically. Pipettes in which debris was visible on the outer surface were rejected.

A 0.5-ml reaction tube was filled with 5 μl of RT reaction buffer containing 1.6× first-strand buffer, 24 mM DTT, deoxynucleotidetriphosphates (dNTPs, 1.2 mM each), 2× hexanucleotide mix (Hoffman-La Roche), and 3 pmol of oligo(dT) primer. The contents of the pipette (≈8 μl) were then expelled into the reaction tube by continuous positive pressure (≈4 bar, filtered N_2). At the end of the expelling procedure, the pipette tip was gently broken to completely empty the pipette by short pressure pulses. The RT reaction was then initiated by adding 100 units of SuperScript II and 20 units of RNasin (both Invitrogen). After incubation for >2 h at 37°C and 1 h at 42°C, cDNA was ethanol-precipitated in the presence of 1 μg of glycogen (Ambion), 250 ng of poly(C) RNA (Amersham Biosciences), and 250 ng of poly(dC) DNA (Amersham) with 0.1 vol 3 M NaAc (pH 4.8) and 3.3 vol ethanol at −20°C overnight and a subsequent centrifugation (4°C, 20,000 × g, 50 min). Supernatant was replaced by 100 μl of 75% ethanol, followed by a second centrifugation (4°C, 20,000 × g, 20 min). After removal of the supernatant, the cDNA pellet was dried at 45°C and resuspended in 39.6 μl of sterile water (Sigma).

PCR analysis was performed in two steps, a first round of multiplex PCR, followed by a second round of specific quantitative PCRs, each with a single primer set. For the multiplex PCR, external primers spanning 225- to 423-bp fragments were designed for an optimal annealing temperature of 53°C by using PrimerExpress 2.0 software (Applied Biosystems). Five microliters of 10× polymerase buffer, 25 mM $MgCl_2$, 1 mM dNTPs (each), 1.5 units of AmpliTaq Gold LD (Applied Biosystems) and 1 pmol of the mixture of external primers were added to the single-cell cDNA solution and amplified the cDNA fragments during a standard temperature cycle protocol (94°C for 5 min, followed by 15 cycles with 94°C for 25 s, 53°C for 35 s, and 68°C for 40 s). qPCR and data analysis were performed as described (10), using 2 μl of the multiplex PCR product as template for each qPCR. The total volume was 25 μl, with 880 nM nested primer (each) and 200 nM TaqMan probe, and amplification was carried out with an ABI Prism 7000 sequence detection system (Applied Biosystems) using a default temperature cycle protocol (50°C for 2 min, 95°C for 10 min, followed by 48 cycles with 95°C for 15 s and 60°C for 1 min). Primers and TaqMan probes were designed by using PrimerExpress 2.0 software (Applied Biosystems) and selected for maximal specificity and intron-overspanning amplicons (Tables S3 and S4). A gene was classified as nonexpressed if the fluorescence signal remained below a threshold of 0.2 units after 48 cycles.

Several control experiments were performed to validate the results of RT-qPCR analysis. Amplification efficiency of qPCR for synaptotagmins 1–15, parvalbumin, and calbindin 1 was assessed by using serial dilutions of brain cDNA (mRNA extraction with TRIzol; Invitrogen; cDNA synthesis as described for single-cell RT); efficiencies per cycle were ≈2.0 for all assays. Amplification efficiency with the external primers was evaluated in a standard PCR with 35 cycles on brain cDNA and subsequent analysis on a 1% agarose-TAE-gel stained with ethidium bromide.

To exclude the possibility of false-positive results, four different types of controls were performed: (*i*) controls in which patch pipettes were inserted into the slice at the position of a previously or subsequently recorded BC with maintained positive pressure ($n = 6$); (*ii*) controls in which patch pipettes were inserted into the slice as in *i*, but positive pressure was reduced ($n = 1$); (*iii*) controls in which patch pipettes were positioned above the slice, and bath solution was harvested by application of suction for several seconds ($n = 2$); and (*iv*) controls in which cytoplasm was harvested normally, but reverse transcriptase was omitted ($n = 2$). RT-qPCR procedures for the controls were identical to those for single-cell analysis. All controls gave consistently negative results for the entire set of genes examined in this study.

1. Stoppini L, Buchs PA, Muller D (1991) A simple method for organotypic cultures of nervous tissue. *J Neurosci Methods* 37:173–182.
2. Geppert M, *et al.* (1994) Synaptotagmin I: A major Ca^{2+} sensor for transmitter release at a central synapse. *Cell* 79:717–727.
3. Geiger JRP, Lübke J, Roth A, Frotscher M, Jonas P (1997) Submillisecond AMPA receptor-mediated signaling at a principal neuron–interneuron synapse. *Neuron* 18:1009–1023.
4. Kraushaar U, Jonas P (2000) Efficacy and stability of quantal GABA release at a hippocampal interneuron–principal neuron synapse. *J Neurosci* 20:5594–5607.
5. Barrett EF, Stevens CF (1972) The kinetics of transmitter release at the frog neuromuscular junction. *J Physiol (London)* 227:691–708.
6. Efron B, Tibshirani RJ (1998) *An Introduction to the Bootstrap* (Chapman and Hall/CRC, London).
7. Hefft S, Jonas P (2005) Asynchronous GABA release generates long-lasting inhibition at a hippocampal interneuron–principal neuron synapse. *Nat Neurosci* 8:1319–1328.
8. Jonas P, Major G, Sakmann B (1993) Quantal components of unitary EPSCs at the mossy fibre synapse on CA3 pyramidal cells of rat hippocampus. *J Physiol (London)* 472:615–663.
9. Clements JD, Bekkers JM (1997) Detection of spontaneous synaptic events with an optimally scaled template. *Biophys J* 73:220–229.
10. Aponte Y, Lien CC, Reisinger E, Jonas P (2006) Hyperpolarization-activated cation channels in fast-spiking interneurons of rat hippocampus. *J Physiol (London)* 574:229–243.
11. Monyer H, Jonas P (1995) Polymerase chain reaction analysis of ion channel expression in single neurons of brain slices. In *Single-Channel Recording*, eds Sakmann B, Neher E (Plenum, New York), 2nd Ed, pp 357–373.

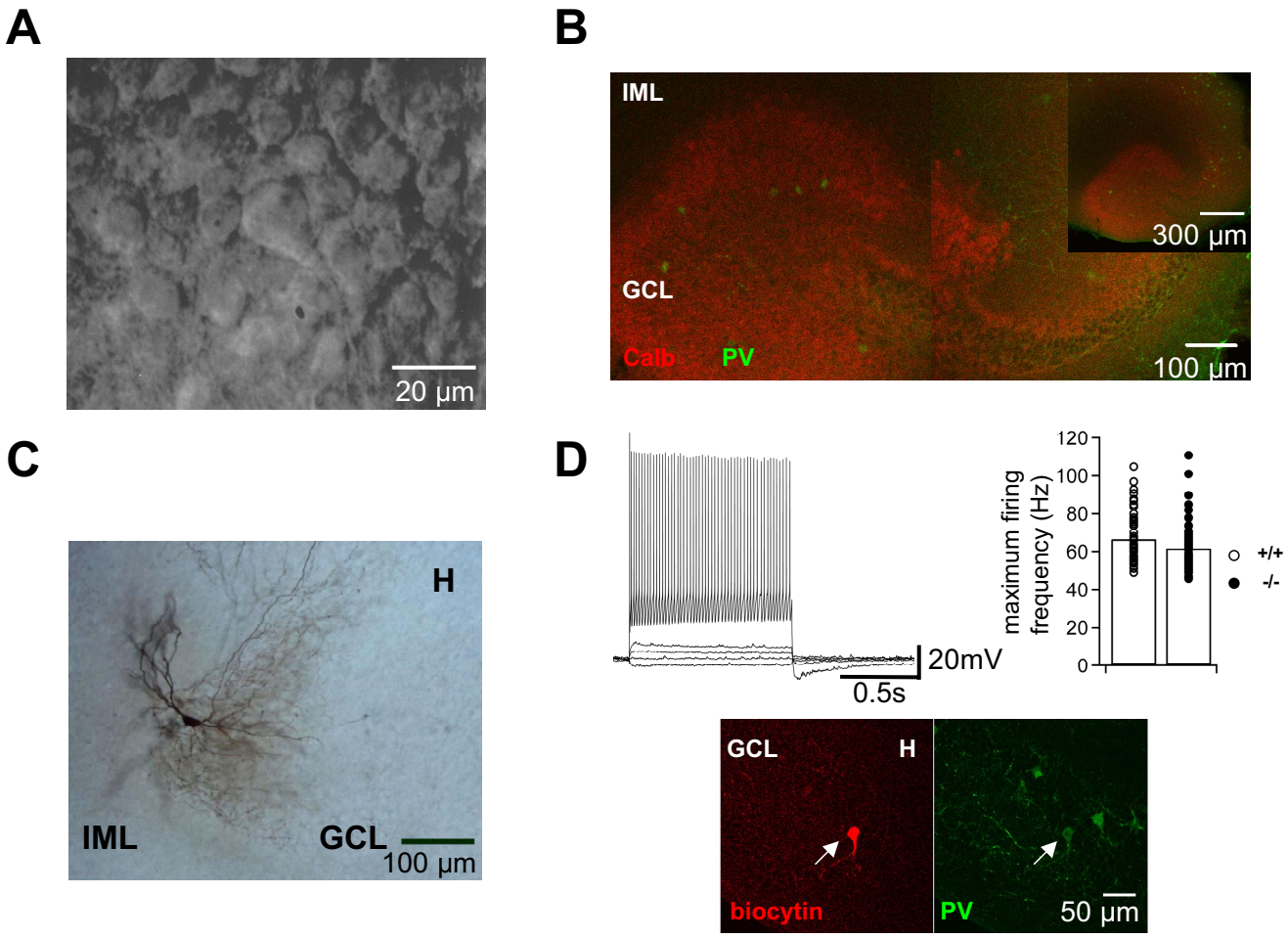

Fig. S1. Morphological properties and identification of fast spiking, parvalbumin-expressing BCs in organotypic slice cultures. (*A*) Infrared differential interference contrast videomicrograph of a BC in a knockout hippocampal slice culture (18 DIV). The BC (*Center*) can be distinguished from adjacent granule cells by the large triangular soma. (*B*) Confocal image of the hippocampus in an organotypic slice culture. BCs were labeled with an antibody against parvalbumin (Alexa Fluor 488-conjugated secondary antibody), GCs with an antibody against calbindin (Alexa Fluor 568-conjugated secondary antibody). Note that the basic morphology of the trisynaptic circuit is preserved. (*C*) Photomicrograph of a biocytin-labeled BC in the dentate gyrus visualized using 3,3′-diaminobenzidine as a chromogen. Note the axonal arborization in the granule cell layer. (*D*) Fast spiking AP phenotype of BCs in organotypic slice culture. (*Upper Left*), voltage responses evoked by 1-s current pulses of −100 pA, 0, 100 pA, 200 pA, and 2,000 pA amplitude. (*Upper Right*), summary bar graph of maximum average AP frequency for BCs in wild-type and knockout mice (74 and 62 BCs, respectively). Bars represent mean values, circles show data from individual experiments. (*Lower*) Parvalbumin immunoreactivity of a previously recorded BC (arrow). Data in *A* and *D Left Upper* were obtained from the same cell. GCL, granule cell layer; IML, inner molecular layer; H, hilus.

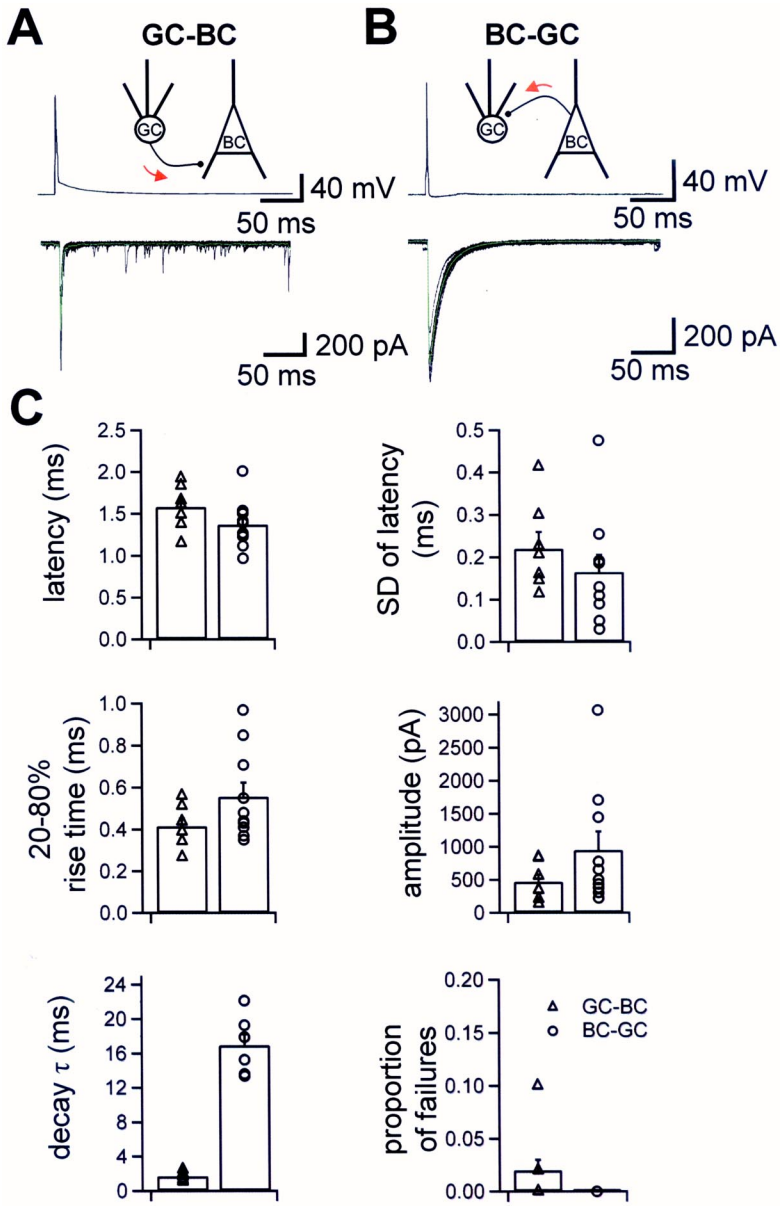

Fig. S2. Basic functional properties of BC–GC and GC–BC synapses in organotypic slice cultures from wild-type mice. (*A*) Unitary EPSCs at the GC–BC synapse. Upper traces, presynaptic APs; lower traces, 10 consecutive EPSCs (black) and superimposed average EPSC (green). (*B*) Unitary IPSCs at the BC–GC synapse. Upper traces, presynaptic APs; lower traces, 10 consecutive IPSCs (black) and superimposed average IPSC (green). (*C*) Summary bar graph of latency, SD of latency as a measure of temporal precision of release, 20–80% rise time, peak amplitude, decay time constant of PSCs (decay τ), and percentage of failures in excitatory GC–BC synapses (triangles) and inhibitory BC–GC synapses (circles). Note that functional properties of evoked GC–BC EPSCs and BC–GC IPSCs are similar to those reported previously in acute rat hippocampal slices (3, 4). Data from 5 GC–BC pairs and 22 BC–GC pairs.

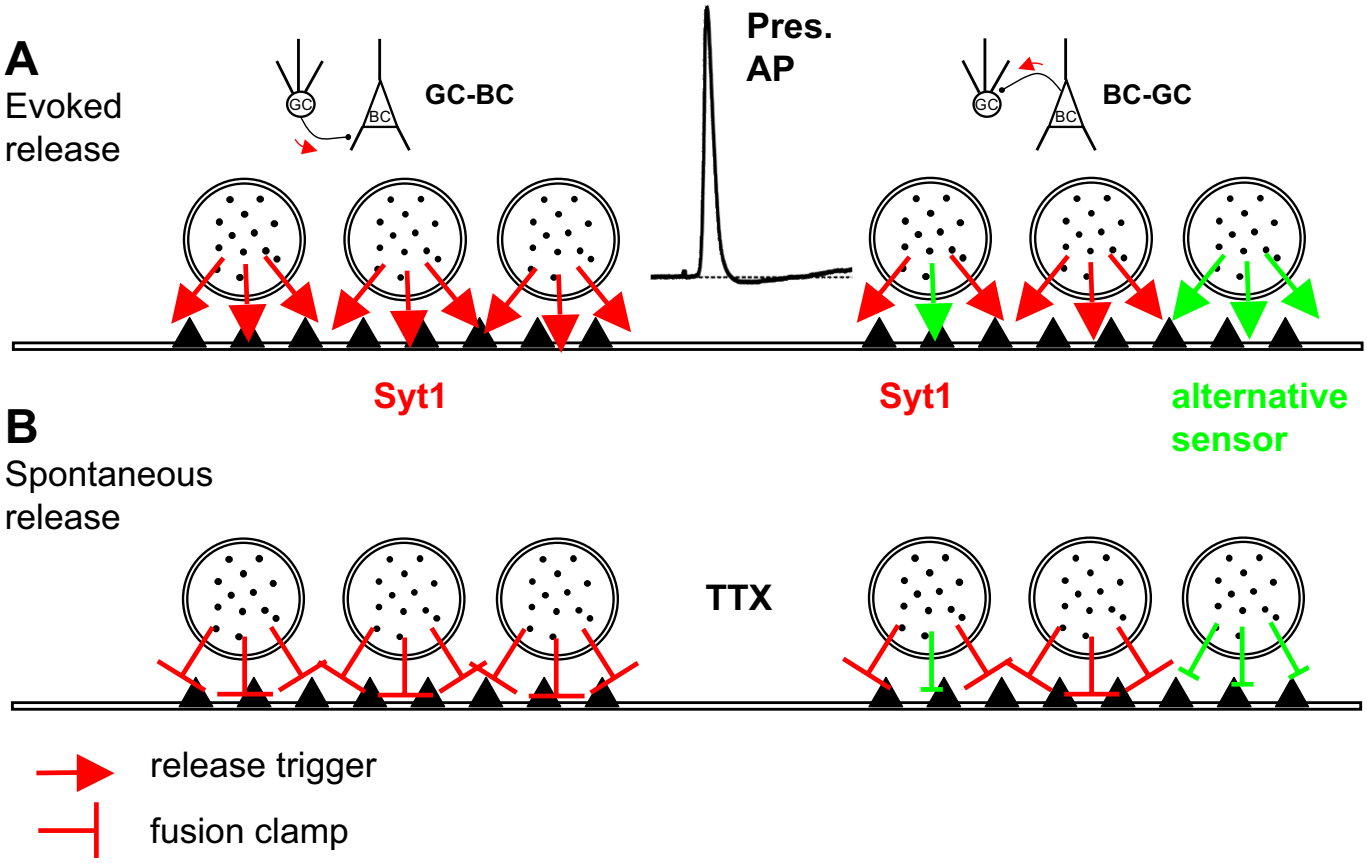

Fig. S3. Hypothetical view of the differential contribution of synaptotagmins at excitatory GC–BC and inhibitory BC–GC synapses. (*A*) Evoked transmitter release after single APs. Triangles indicate the active zone, circles represent synaptic vesicles. Syt1 is indicated in red, the alternative Ca^{2+} sensor (probably another synaptotagmin) in green. The arrows indicate the facilitatory effect of synaptotagmins on fusion. At excitatory GC–BC synapses (*Left*), Syt1 is the only Ca^{2+} sensor. Thus, synchronous release is abolished in Syt1-deficient mice. At inhibitory BC–GC synapses (*Right*), Syt1 and another synaptotagmin are present, either on the same individual vesicle or on different vesicles. Thus, synchronous release is maintained in Syt1-deficient mice, but release probability is reduced. (*B*) Spontaneous transmitter release in the absence of APs after TTX application. The T-bars indicate a postulated inhibitory effect of synaptotagmins (fusion clamp) under these conditions. At excitatory GC–BC synapses, Syt1 is the only synaptotagmin, whereas at inhibitory BC–GC synapses, Syt1 and another synaptotagmin coexist. However, the spontaneous release rate is increased at both synapses after genetic elimination of Syt1, because the alternative synaptotagmin has a weaker clamping efficiency than Syt1 (represented by the shorter arms of T-bars).

Table S1. Comparison of evoked transmission at excitatory GC–BC and inhibitory BC–GC synapses in wild-type and synaptotagmin 1-deficient mice

	GC–BC EPSCs wild-type, mean ± SEM [range] (*n*)	GC–BC EPSCs knockout, mean ± SEM [range] (*n*)	BC–GC IPSCs wild-type, mean ± SEM [range] (*n*)	BC–GC IPSCs knockout Mean ± SEM [range] (*n*)
Latency of PSC[a]	1.58 ± 0.10 ms	–	1.34 ± 0.05 ms	1.37 ± 0.06 ms
	[1.15–1.92] (7)	–	[0.97–2.01] (22)	[0.99–2.50] (28)
20–80% rise time of PSC	0.41 ± 0.04 ms	–	0.53 ± 0.03 ms	0.48 ± 0.02 ms
	[0.27–0.56] (7)	–	[0.35–0.97] (22)	[0.30–0.75] (28)
Peak amplitude of PSC (including failures)	468 ± 108 pA	–	688 ± 142 pA	455 ± 92 pA
	[135–845] (7)	–	[141–3068] (22)	[116–2471] (28)
Decay τ of PSC[b]	1.68 ± 0.19 ms	–	16.3 ± 0.7 ms	15.2 ± 0.81 ms
	[1.09–2.47] (7)	–	[11.1–22.1] (16)	[8.4–21.3] (22)
Percentage of failures (2 mM Ca^{2+}, 1 mM Mg^{2+})[c]	2 ± 1%	–	1 ± 1%	5 ± 1%
	[0–10] (7)	–	[0–13] (22)	[0–26] (28)
PSC_{10}/PSC_1 of average PSCs	0.13 ± 0.03	–	0.19 ± 0.02	0.54 ± 0.05
	[0.05–0.27] (7)	–	[0.07–0.24] (10)	[0.14–0.76] (12)
Decay τ of synchronous release period[d]	–	–	0.33 ms	0.28 ms
	–	–	(5)	(4)
Initial asynchronous release rate[e]	0.02 ± 0.01 quanta ms^{-1}	0.06 ± 0.02 quanta ms^{-1}	0.08 ± 0.02 quanta ms^{-1}	0.06 ± 0.02 quanta ms^{-1}
	[-0.004–0.07] (10)	[0.03–0.12] (8)	[0.02–0.21] (9)	[0.01–0.15] (9)
Decay τ of asynchronous release[f]	171 ± 61 ms	195 ± 31 ms	64.7 ± 8.3 ms	188 ± 78 ms
	[29–258] (10)	[101–290] (8)	[34.7–112.4] (9)	[25–717] (9)
No. of synchronous quanta during train[g]	10.7 ± 1.9	−0.32 ± 0.36	51.0 ± 13.8	24.4 ± 4.6
	[3.1–18.1] (10)	[−1.54–−0.81] (8)	[11.4–144.1] (9)	[9.2–43.1] (9)
No. of asynchronous quanta during train[g]	4.16 ± 2.28	6.83 ± 2.34	18.3 ± 6.3	12.4 ± 2.9
	[-2.4–13.5] (10)	[2.25–15.4] (8)	[1.52–52.11] (9)	[2.6–29.4] (9)
No. of asynchronous quanta after train[h]	4.36 ± 3.00	9.98 ± 3.65	4.50 ± 2.00	5.5 ± 1.8
	[−1.9–21.3] (10)	[2.41–22.6] (8)	[−1.08–15.88] (9)	[−1.6–16.5] (9)
Total no. of quanta during and after train	19.2 ± 4.5	16.5 ± 5.5	73.8 ± 16.9	42.3 ± 8.2
	[8.9–43.6] (10)	[7.8–34.6] (8)	[15.1–183.3] (9)	[16.8–82.2] (9)

[a]The latency was measured from the steepest point of the rising phase of the presynaptic AP to the onset of the synaptic event.
[b]The decay time constant was determined by fitting sweeps with a single exponential.
[c]Events were classified as failures when the amplitude was less than two times the standard deviation of the baseline noise.
[d]The decay phase of the time course of release (determined from the first latency distribution) was fitted with a single exponential.
[e]Calculated as the maximum amplitude of a single exponential fitted to the decaying phase of asynchronous release after a 50-Hz train of 10 APs
[f]The decaying phase of asynchronous release was fitted with a single exponential.
[g]In these experiments, a 50-Hz train of 10 APs was used as stimulus.
[h]Asynchronous release after the train was calculated starting 20 ms after the end of the presynaptic AP train.

Table S2. Sequences of primers used for mouse genotyping

Primer	Sequence
Neo-fwd	CTT GGG TGG AGA GGC TAT TC
Neo-rev	AGG TGA GAT GAC AGG AGA TC
Synaptotagmin 1-fwd	GAG AAA CTG GGT GAC ATC TG
Synaptotagmin 1-rev	TCA GAT AAG CCA CCC ACA TC
Control-fwd	CAA ATG TTG CTT GTC TGG TG
Control-rev	GTC AGT CGA GTG CAC AGT TT

Table S3. Sequences and location of primers used for RT-qPCR experiments in acute slices from rats

Gene	GenBank accession no.	SDS-fwd	SDS-rev	TaqMan	ext-fwd	ext-rev
Parvalbumin	NM_022499 bzw. CF977249	PV-63F AAGTTGCAGGATGTCGAT-GACA	PV-147R GAAGGAGTCTGCAGCAGTA-AAGG	PV-94T TCGCCTTCTTGATGTCCT-CAGCGCT	PV-10F 4 TTTCGCACTTGCTCTGC	PV-273R3 AATGGACCCCAGCT-CATC
Calbindin1	NM_031984	Calbindin1–387F GGAGCTGCAGAACT-TGATCCA	Calbindin1–481R CATATTGATCCA-CAAAGGTTTTCATC	Calbindin1–416T TCCAGCCTTCTT-TCGTGCCTGCA	Calbindin1–297F CCACCTGCAGT-CATCTCTG	Calbindin1–560R AAGAGCAG-CAGGAAATTCTC
Syt1	NM-001033680	Syt1–948F ACTGGGAAAGCTCCAATAT-TCACT	Syt1–1072R CTTTGACGTATGGATCG-GATGTAC	Syt1–990T ATGATTCCCACCAA-CAGCTGGTTA	Syt1–819F GAACGCCATTAACAT-GAAAG	Syt1–1189R TGCCACCTAATTC-CGAGTA
Syt2	NM_012665	Syt2–1136F ATGAGTCATTCAGCTTC-GAGATCC	Syt2–1239R TCCGATGGCTTCATTCTTGC	Syt2–1182T CCAGGTGGTCGTCAC-CGTGCTAGACTAT	Syt2–948F TACCTCCTTGCGCTACGT	Syt2–1370R CCCAGAAGAGCATC-CACTT
Syt3	NM_019122	Syt3–208F TTCAACGAACTGCGAAT-CAGA	Syt3–319R GAGAGACACCCAAGAG-GACGAT	Syt3–260T CCGTGAGCCTGCTGT-CAGTCATCG	Syt3–74F TAAGCACAGTGTAGGAT-CACG	Syt3–341R CACAACTTCCAGGA-CACGA
Syt4	NM_031693	Syt4–257F ACGCAGAAAACATG-GCTCCT	Syt4–344R AGGCCAAAAGCACTGAA-GATG	Syt4–278T TCACCACCAGCCGCGTG-GAAT	Syt4–103F GGTGGCACATTGCT-GATAG	Syt4–408R CTTGTTGGACTTAGCG-GATC
Syt5	NM_019350	Syt5–551F TGGGCCGGAGTTACATA-GATAAG	Syt5–651R GCCTAACTGGTGCTTGTC-CAATAC	Syt5–578T AGCCTGAAATAGAG-GAACTGGACCCC	Syt5–460F TGTTTCTGTCTCTACCG-GAAG	Syt5–782R GGCAGCAGATAGA-CACTAACAT
Syt6	NM_022191	Syt6–1422F CTCACCCTCACGGTGAT-CAA	Syt6–1518R GCCCATCACATAGTAGG-GACACT	Syt6–1445T TCGCAATCTCAAAG-CAATGGATATCACG	Syt6–1337F GAAGGACATCCAG-TACGCTACT	Syt6–1656R CTCTGTCATAGTC-CATAACGGA
Syt7	NM_021659	Syt7–234F CCGTCAGCCTTAGCGTCACT	Syt7–319R CAAGGAGTTCTTGTAGCGTT-TGC	Syt7–270T TGTGCCACTGGTGT-CAGCGCA	Syt7–219F2 TCTCTGCAATCATCACCG	Syt7–515R2 AGAGCATGAG-CATCTCGC
Syt8	NM_053325	Syt8–474F CGGGAGAAGACATGAGA-CAAAAG	Syt8–558R TGCTGGTGGGACCAGGAA	Syt8–502T CGTGGGACACTCTGTC-CCATGTTTGA	Syt8–376F GGAAGCCAGGAGATTA-GAGT	Syt8–670R CATGCTGAAGGTCCA-CAGT
Syt9	NM_053324	Syt9–453F CGTCCGTGTACAGCGA-CAAGT	Syt9–553R GTTGGATATTAAAGTC-CGGGTTTG	Syt9–488T CGTCAGCTCGGCATA-ACTCAATCCGA	Syt9–304F ACTGATACAGAGA-CAAATGAGCA	Syt9–604R ACTCTGGCTTAATTC-TACCAATC
Syt10	NM_031666	Syt10-106F GGCATCTTTCCAGC-CGATAG	Syt10-196R GGCCACAGAAGCTTACAA-CAACT	Syt10-134T AATGTCTGTGCCACCTC-CGCCCT	Syt10-89F AGTGGGACAAGTGTTCGG	Syt10-313R2 TTGGAGCACTT-GAGATGCT
Syt11	NM_031667	Syt11-1160F AATGACAGTCGTGGTCCT-CAAAG	Syt11-1245R CGTTCACCTTGACATAAG-GATTACC	Syt11-1187T ACACTTGCCGAAGATG-GATATCACC	Syt11-1119F GAACTCCAGGTATCTCT-GTCATAC	Syt11-1388R GTCAATGACAAG-GAACTCGAT
Syt12	NM_138835	Syt12-786F CCTGCTTCATGCGTGTCAGT	Syt12-858R TAGGCATTCCTCTGGATCCG	Syt12-807TCCACGATCTGTTCGTCTG-GCAGCA	Syt12-606F GCAAGTCACAGTCGGCT	Syt12-1005R TCCAGAACAGA-CAGCTTCAG
Syt13	NM_030839	Syt13-965F GGGCCTGAATGGAGCATCT	Syt13-1065R ACAGAAGGACCTC-CCCAGTTC	Syt13-1018T AGACCACAGCAAAG-GAGCCATCTGCA	Syt13-907F TCACCCTGAGGACCTGTG	Syt13-1172R GACAGAGACATCTT-TGCCTAGA
Syt15	NM-181632	Syt15-733F CAGTTTGATGAGAGCT-TCATCTTTCA	Syt15-831R GTGCTTCCTCTGCTTGTT-TACGT	Syt15-780T ACACGGAGAACTTCAG-CACCCTCTGG	Syt15-691F2 CGTTTTCTTCAGTC-CAAGG	Syt15-1009R3 GGAGCACGACCA-CAGTC

Listed are the GenBank accession nos., real-time PCR primers (SDS-fwd and SDS-rev), TaqMan probe, and external primers (ext-fwd and ext-rev) used for each gene. Primers and sequences for RT-qPCR conducted on material harvested from cells in acute slices from rats are given.

Table S4. Sequences and location of primers used for RT-qPCR experiments in slice cultures from mice

Gene	GenBank accession no.	SDS-fwd	SDS-rev	TaqMan	ext-fwd	ext-rev
Parvalbumin	NM_013645	mPV-17F TGCAGGATGTCGATGACA-GAC	mPV-131R TCAGGCCCACCATCTGGA	PV-94T TCGCCTTCTTGATGTCCT-CAGCGCT	PV-10F 4 TTTCGCACTTGCTCTGC	PV-273R3 AATGGACCCCAGCT-CATC
Syt1	NM_009306	mSyt1–983F TTGGCCACGTCACCGAG	mSyt1–1071R GCGGAGGGAGAAGCA-GATG	mSyt1–1003T ic CAGCACTCTG-GAGATCGCGCCA	mSyt1–876F CTCGGAATTAGGTG-GCAA	mSyt1–1120R TCTTGGCTTCCA-GAATGAC
Syt2	NM_009307	mSyt2–1128F ACACAGTGGACCTTG-GCCA	mSyt2–1224R AAGGAGGTACAGATGT-CACCCAAC	mSyt2–1152T ic CGCCTTGTAG-GTCTCTCCATTCCTCGA	mSyt2–1059F TGATGGCAATCTAT-GACTTTG	mSyt2–1337R GCATCAGGTGGATCTTCAC
Syt3	NM_016663	mSyt3–281F ACGAACTGCGGATCA-GAGGATA	mSyt3–390R GAGGGAGACACCCAA-GAGGAC	mSyt3–329T CCGTGAGCCTGCTGT-CAGTCATCG	mSyt3–141F CCACTCTTAAGTAT-AGGATCACGT	mSyt3–410R CACAACTTCCAGGA-CACGA
Syt4	NM_009308	Syt4–257F ACGCAGAAAACATG-GCTCCT	Syt4–344R AGGCCAAAAGCACTGAA-GATG	Syt4–278T TCACCACCAGCCGCGTG-GAAT	Syt4–103F GGTGGCACATTGCT-GATAG	mSyt4–404R CTTGTATGGAG-GAGTCTTGTTG
Syt6	NM_018800	mSyt6–1149F AGGACATCCAGTACGC-TACTAGTGAA	mSyt6–1272R ATTGCTTTGAGATTTC-GACACTTG	mSyt6–1219T CACAGCAGGCAGGCT-CACCCTCA	mSyt6–976F CACCTTTGAT-GAGAACTTCCA	mSyt6–1287R TAGCCTGTGATGTC-CATTG
Syt10	NM_018803	mSyt10–482F AAACAACCGAGC-CTACGTCTTC	mSyt10–582R TTCAGTGCCCACGCTA-AAGTC	mSyt10–534T ACCAAGGCAAAT-GAATGTCTCCAGCGT	mSyt10–461F AACATGCTCGAGTG-CAAAG	mSyt10–705R AAGTTTCCCACAG-GTCTTGA

Listed are the GenBank accession nos., real-time PCR primers (SDS-fwd and SDS-rev), TaqMan probe, and external primers (ext-fwd and ext-rev) used for each gene. Primers and sequences for RT-qPCR conducted on material harvested from cells in organotypic slice cultures from wild-type and knockout mice are given.